

## Applications of high-speed digital pulse acquisition and software-defined electronics (SDE) in advanced nuclear teaching laboratories

F. D. Becchetti, N. Damron and R. O. Torres-Isea

Citation: [American Journal of Physics](#) **88**, 70 (2020); doi: 10.1119/1.5125128

View online: <https://doi.org/10.1119/1.5125128>

View Table of Contents: <https://aapt.scitation.org/toc/ajp/88/1>

Published by the [American Association of Physics Teachers](#)

---

### ARTICLES YOU MAY BE INTERESTED IN

[Why are complex numbers needed in quantum mechanics? Some answers for the introductory level](#)

[American Journal of Physics](#) **88**, 39 (2020); <https://doi.org/10.1119/10.0000258>

[Electric field lines of relativistically moving point charges](#)

[American Journal of Physics](#) **88**, 5 (2020); <https://doi.org/10.1119/10.0000189>

[Reflections in a moving mirror](#)

[American Journal of Physics](#) **88**, 46 (2020); <https://doi.org/10.1119/10.0000172>

[Conservative numerical methods for nonlinear oscillators](#)

[American Journal of Physics](#) **88**, 60 (2020); <https://doi.org/10.1119/10.0000295>

[Using Kepler's laws and Rutherford scattering to chart the seven gravity assists in the epic sunward journey of the Parker Solar Probe](#)

[American Journal of Physics](#) **88**, 11 (2020); <https://doi.org/10.1119/10.0000145>

[Determination of permeability using a classic Darcy water column](#)

[American Journal of Physics](#) **88**, 20 (2020); <https://doi.org/10.1119/10.0000296>

---





# INSTRUCTIONAL LABORATORIES AND DEMONSTRATIONS

The downloaded PDF for any paper in this section contains all the papers in this section.

John Essick, *Editor*

*Department of Physics, Reed College, Portland, OR 97202*

Articles in this section deal with new ideas and techniques for instructional laboratory exercises, for demonstrations and for equipment that can be used in either. Although these facets of instruction also appear in regular articles, this section is for papers that primarily focus on equipment, materials and how they are used in instruction.

Manuscripts should be submitted using the web-based system that can be accessed via the *American Journal of Physics* home page, <http://web.mit.edu/rhprice/www>, and will be forwarded to the ADN editor for consideration.

## Applications of high-speed digital pulse acquisition and software-defined electronics (SDE) in advanced nuclear teaching laboratories

F. D. Becchetti, N. Damron, and R. O. Torres-Isea

*Department of Physics, University of Michigan, Ann Arbor, Michigan 48109*

(Received 14 December 2018; accepted 8 August 2019)

There is a new generation of high-speed programmable pulse digitizers available now from several vendors at modest cost. These digitizers in tandem with on-board or post-processing software combine to produce a Software-Defined Electronics (SDE) system that can be effectively used in several advanced physics teaching lab experiments. In particular, as we will demonstrate, they are particularly well suited for nuclear-physics related experiments, often replacing many analog electronics modules. Appropriate on-board SDE can generate full or partial integrals of the pulses, pulse-shape characterization (PSD) data, coincidence signal indication, fast timing, or other information. Likewise, external PC-based SDE post-processing software can readily be developed and applied by undergraduate students or instructors using one of several different software languages available: MATLAB, PYTHON, LABVIEW, ROOT, BASIC, etc. As demonstrated here, an SDE-based system is a cost-effective substitute for many dedicated NIM or CAMAC electronics modules as this requires only a single digitizer module and a computer. A single digitizer with SDE is easily adapted for use in many different experiments. Applications of various high- and low-speed digitizers with SDE for many other types of physics teaching lab experiments will also be discussed. © 2020 American Association of Physics Teachers.

<https://doi.org/10.1119/1.5125128>

### I. INTRODUCTION

Progress in modern, fast electronics has made many new modes of physics data acquisition possible. In particular, high-speed pulse digitizers with embedded field-programmable gate arrays (FPGAs) are rapidly replacing more conventional discrete, single-function NIM and CAMAC modules in many physics research experiments. In addition, as costs for these digitizer units continue to fall, they become attractive and affordable for use in advanced physics teaching laboratories, and in particular for many nuclear experiments.<sup>1-3</sup> While NIM and CAMAC electronics, along with analog or digital oscilloscopes, are still useful as teaching tools for some initial experiments, the use of a pulse digitizer and related software-defined electronics (SDE), which students or instructors can program if appropriate, introduces students to modern state-of-the-art physics research instrumentation and methods.

The on-board FPGAs and basic SDE software typically included with these digitizers can be used to initially display the pulse waveforms, gating signals, and timing signals in

digital storage oscilloscope mode (DSO), and then display the pulse integral spectra as well as basic pulse-shape information. This information can be recorded and analyzed directly or the digitizer module can be programmed to produce other outputs suitable for user-written SDE. The experiments described here use primarily student- or instructor-written SDE, with vendor-supplied basic SDE used mainly to monitor the real-time data acquisition. Alternately, the digitizer vendors or their user groups often can supply the necessary post-processing SDE software. As we wish to demonstrate, adapting pulse digitizers and related SDE for data acquisition and analysis in physics teaching labs (and in particular advanced nuclear labs) has the following advantages over past methods using arrays of modular electronics and instruments:

- (1) As noted, it introduces students (and in some cases also instructors) to modern state-of-the-art experimental physics research instrumentation and methods.
- (2) Students can be actively involved in programming the digitizers via the on-board FPGAs including specifying the type of data output. This requires student

understanding of the data needed, e.g., pulse height, pulse integral, time of flight, pulse-shape discrimination, coincident events, etc., and to set the appropriate digitizer parameters.

- (3) Students can apply and reinforce programming skills they have acquired, or readily learn what is needed, to create SDE to process and visualize the digitized pulse data.
- (4) The data can be acquired in a multi-parameter mode allowing for highly educational 2D or 3D data visualization, especially for coincident events. This is not easy to achieve with conventional modular electronics.
- (5) One digitizer can be used for several different types of experiments, often eliminating many of the specialized electronics modules needed for specific experiments (e.g., NIM or CAMAC modules and their power-supply crates). There can be considerable cost savings, in many cases, if one is buying new equipment. In addition, the designs of many NIM and CAMAC modules are old and contain internal components that are difficult to replace.
- (6) Several digitizers can be configured for a single experiment. Thus, depending on the number of detection systems available, several groups of students can simultaneously perform the identical experiment, e.g., for a studio type lecture-lab course.
- (7) Likewise, most digitizers can also be used as a high-speed SDE digital storage oscilloscope (DSO) replacing a conventional or digital oscilloscope. The multi-channel DSO mode is very instructive both for observing detector signals prior to digitization and facilitating the determination of FPGA parameters.
- (8) Better and more extensive data can usually be obtained compared to older methods. One can then often use radioactive sources with less strength and in particular low-cost US-NRC “exempt” quantity sources.
- (9) Most digitizers can be operated remotely, via Ethernet connections or other protocols. This permits students to run and control experiments remotely, permitting extended run times such as overnight runs or runs between lab periods. This again often facilitates the use of low intensity, US-NRC “exempt” radioactive sources or if using strong sources, can minimize students’ exposure to nuclear radiation.
- (10) The same SDE modules can usually be shared among several similar digitizers.
- (11) The digitizers readily permit open-ended student-originated experiments, including undergraduate honors theses and independent research and, also, graduate-level research, without need to purchase new, specialized electronics modules.

Although many suitable commercial digitizers exist and many new ones are being introduced on a regular basis, we will describe in more detail the use of the CAEN DT5790N module,<sup>1</sup> which is particularly well suited for advanced nuclear-physics teaching labs (Fig. 1). This unit consists of a two-channel high-speed digitizer (12 bits, 250 MS/s) conveniently combined with two programmable short-protected HV detector power supplies (4 kV max, 4 W each, SHV outputs) together with 12V 100 mA and 24V 50 mA low voltage supplies (DB9 outputs) suitable for preamps, etc. Like many digitizers, it can be controlled remotely, in this case via built-in Ethernet, USB, or fiber-optic interfaces. This permits

students to run and monitor experiments over long running periods beyond a normal lab session, especially when using low-intensity radioactive sources.

Another suitable stand-alone commercial digitizer with four 12-bit, 250 MS/s inputs (however no kV HV supplies) is the XIA PIXIE-Net.<sup>2</sup> Both the CAEN and XIA digitizers are modestly priced (\$4k–6k depending on options) and include extensive, user-friendly on-line operating manuals,<sup>1,2</sup> which facilitate operation and programming the on-board FPGAs including specifying the format of the digitized output data. Both CAEN and XIA provide good technical support and have a large user base as both produce digitizers are widely used in physics research. As with the CAEN digitizers, XIA provides a number of SDE programs in C or LABVIEW<sup>4</sup> that can be used with their digitizers.

Our particular CAEN unit (DT5790N) has two negative HV outputs suitable for most scintillator+photo-multiplier (PMT) detectors but can also be used to power other nuclear detectors using negative bias voltage. (The DT5790P model has positive HV supplies.) A lower-cost version (<\$5k) of this digitizer is available (CAEN DT5720) without the built-in power supplies but otherwise is similar and software compatible with the DT5790 for use with SDE. Like the XIA digitizer, the 5720 unit also is available as a four-channel digitizer.<sup>1</sup> Although CAEN makes a digitizer-based teaching module utilizing a DT5720 digitizer (CAEN SP5600<sup>1</sup>), this module is primarily designed for experiments demonstrating the use of small-area silicon PMTs. Hence, it has more limited applications than the DT5790/5720 and XIA PIXIE-Net digitizers described here. Likewise, there are many other companies producing research-grade high-speed digitizers but most of these at this writing have more than four channels and usually require a special power-supply crate, which makes them expensive for teaching purposes.

We have configured a DT5790N digitizer together with suitable custom SDE software, mostly written by an undergraduate student (ND), for several important nuclear physics experiments typically done in advanced physics teaching labs:<sup>5–10</sup> Gamma-Gamma Coincidence (Na-22 and Co-60 sources), Compton Scattering, Muon and Nuclear Decay Lifetimes, and Fission-Neutron Time-of-Flight, with additional experiments planned. Students or instructors, even those with minimal programming experience, can generate the needed SDE as part of a given experiment. Sample SDE programs used here, as noted mostly written in Python by a senior University of Michigan (UM) undergraduate student (co-author N.D.), and related information can be found in Ref. 43. However, the CAEN DT5720 unit is compatible with CAEN’s CoMPASS vendor-supplied SDE software<sup>1</sup> so that is another option. (It is anticipated that CAEN will soon

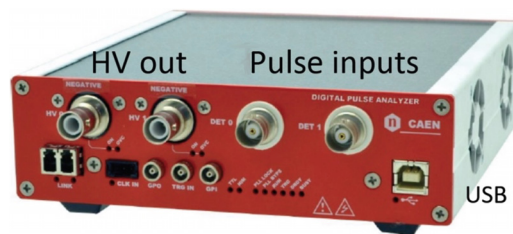


Fig. 1. Picture of the CAEN DT5790N digital pulse analyzer/HV supply unit showing inputs and outputs (12 V and 24 V DB9 outputs in back, not shown).



have a version of CoPASS SDE software useable with the DT5790 digitizers.)

Most of the experiments described here are normally performed with modular NIM or CAMAC electronics and 1D multi-channel analyzers (MCAs). Such experiments are described in several commercial lab manuals,<sup>5-7</sup> in various on-line advanced lab write ups (e.g., Refs. 8 and 9), or in relevant textbooks.<sup>10</sup> The underlying nuclear physics being studied is covered in detail in many physics' textbooks.<sup>11-14</sup> Other physics teaching lab applications that can utilize lower-speed low-cost digitizers and SDE will also be described. A specific experiment developed with one particular low-cost modest-speed digitizer (Red Pitaya<sup>3</sup>) will be used as an example.

## II. HIGH-SPEED DIGITIZED PULSE INFORMATION

In this paper, we primarily discuss applications of high-speed digitizers such as the CAEN and XIA units, which we define as having greater than 200 MS/s sampling rate. Such speed, which corresponds to  $<5$  ns resolution, is often needed for nuclear experiments,<sup>5-10</sup> including particle time-of-flight, fast coincidence measurements, pulse-shape discrimination (PSD), and other experiments using scintillators, solid-state Si or Ge detectors.

The digitizer unit used here (CAEN DT5790N<sup>1</sup>) was purchased with FPGA software options appropriate for identifying and generating charged ion, neutron, electron, muon, or gamma-ray signals from one or two scintillators, either organic plastic or organic liquid scintillators, inorganic scintillators, as well as various solid-state or gaseous detectors. The XIA PIXIE-Net digitizer has similar options.<sup>2</sup> The CAEN 5790N digitizer has suitable remote-controlled HV detector power supplies, and includes two on-board programmable FPGAs to do specific user-defined or CAEN-software defined on-board SDE pulse analysis (Fig. 2). Again, the latter also applies to the XIA digitizer.

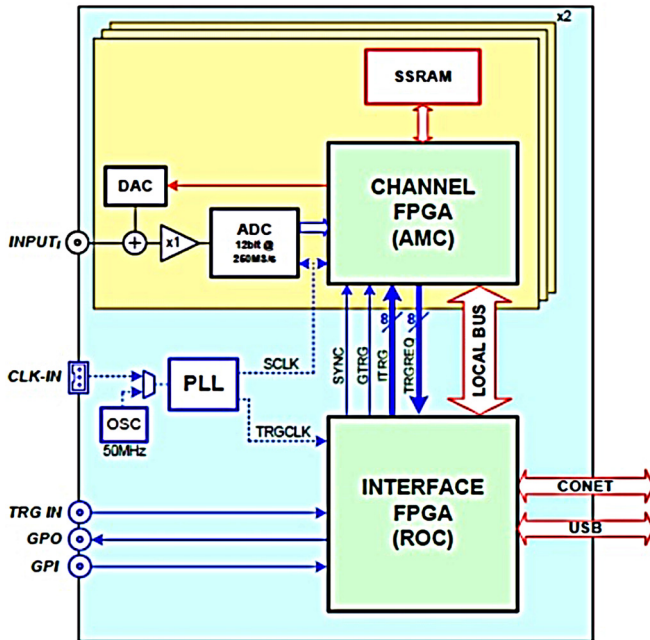


Fig. 2. On-board module layout of the CAEN DT5790 digitizer for one of the two channels (HV and preamp power supply circuits not shown). DAC = digital-to-analog converter; ADC = analog-to-digital converter; PLL = phase-locked loop; FPGA = field-programmable gated array.

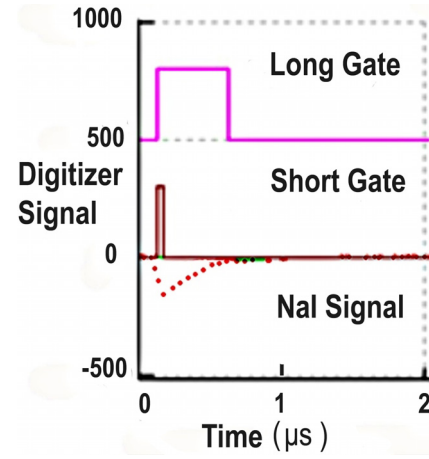


Fig. 3. Pulse digitization display (SDE DSO mode) showing the long (Q long) and short (Q short) pulse-integral gates used for a typical NaI(Tl) detector gamma-ray signal (PMT anode).

Examples of digitized pulse data from a scintillator PMT anode pulse observed using the DT5790N digitizer's SDE DSO mode are shown in Fig. 3 and Sec. III. In most plastic scintillators, there is no pulse-shape discrimination (PSD) but one can then use the time-stamped data from the digitizer (Fig. 4) to determine the signal timing (in this unit to 4 ns accuracy). The fast timing can be used between two scintillator signals to separate gamma rays from neutrons (or charged ions) via their time-of-flight (ToF) as determined with a user-defined SDE Time-to-Digital Converter (SDE TDC) in post processing or, e.g., using CAEN's CoPASS software if using the DT5720 unit. Similarly, with a SDE 2D-Multi-channel Analyzer (SDE 2D MCA), as an example for gamma-gamma coincidence measurements (see below), one typically just integrates the digitized pulses from two detectors with coincidence/non-coincidence signals generated in the on-board FPGA or alternately generated in SDE in post-processing using the time-stamped list data (Fig. 4). However, pulse pile-up rejection (PUR) often must also be

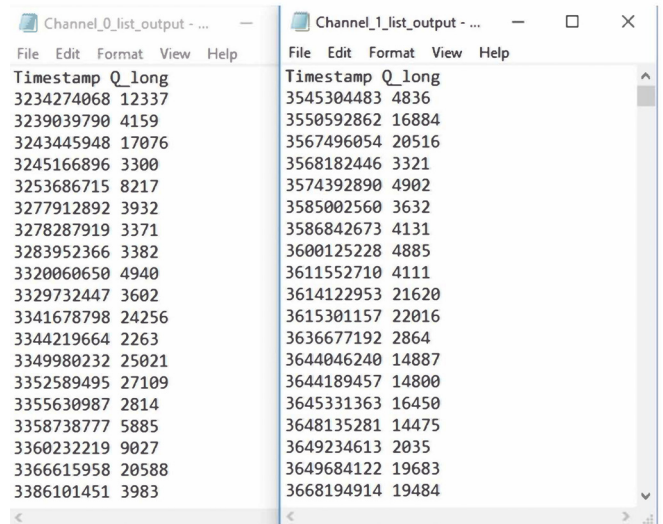


Fig. 4. Sample of list-mode data files generated in the data acquisition computer for two detectors having coincident gamma-ray signals. Shown are the time stamps (in 4 ns intervals) and the integrated scintillator pulse values (Q long, Fig. 3).

employed when using intense sources to avoid false coincident events (see below). As noted, the CAEN DT5720 and XIA units operate in a similar fashion but lack the built-in HV supplies. Likewise, the XIA PIXIE-Net unit has similar user-defined software options for displaying and generating digitized pulse information via the on-board FPGA<sup>2</sup> and has many of the same features of the CAEN units.

Most fast pulse digitizers have a limited input pulse voltage maximum, in the case of the DT5790 and DT5720 units,  $\pm 2$  V maximum and, for the XIA unit,  $\pm 3.5$  V. However, it is sometimes desirable to obtain optimal signal-to-noise performance from a PMT (or other detector) and thus run these detectors at their specified optimum operating voltage. This may produce signals outside the range of the digitizer. In such cases precision GHz-bandwidth 50  $\Omega$  in-line attenuators<sup>15</sup> can be used, and often are needed, to match the digitizer pulse voltage input limits. This is often preferable to lowering the PMT voltage well beyond the specified operating voltage to reduce the input signal voltage.

Below we illustrate the use of SDE software as applied to advanced undergraduate teaching-laboratory nuclear experiments with the key SDE modules indicated.

### III. EXPERIMENTS WITH HIGH-SPEED DIGITIZERS AND SDE

#### A. Na-22 coincident positron-annihilation radiation (SDE 2D MCA and TDC)

The proton-rich radioactive nucleus Na-22 (2.6 year half-life) preferentially decays to the stable nucleus Ne-22 first via positron emission or electron capture to the 1.27 MeV first excited state in Ne-22 (see Ref. 6, Expt. 13). This state then decays via gamma emission to the Ne-22 ground state. The positrons emitted then annihilate in the source by combining with an atomic electron, producing primarily two back-to-back 511 keV gamma rays in coincidence.<sup>10</sup>

The set up for detecting the two coincident positron-decay gammas typically consists of two scintillator+PMT detectors.<sup>5–10</sup> Fast coincidence timing usually is best done using plastic scintillators, but owing to their low effective atomic number  $Z$ , as they are organic, they do not produce photo-peaks at well-defined energies,<sup>10</sup> in this case, 511 keV. Instead they produce non-distinct Compton spectra extending out to the Compton maximum energy (about 341 keV). NaI(Tl) scintillators are thus preferred to measure gamma energy spectra as these produce full-energy photo-peaks. They are considerably slower (about 10 times slower) than plastic for coincidence timing<sup>10,16,17</sup> but their response time is adequate for this experiment.

We have used two NaI(Tl) detectors with the CAEN DT5790N digitizer and a student-written SDE 2D multi-channel analyzer (SDE 2D MCA) module. The latter can confirm that the two Na-22 positron-annihilation gammas occur in fast coincidence, each with energy 511 keV, and occur back-to-back, i.e.,  $180^\circ$  apart. This is required to conserve momentum as the positron annihilates with an electron in the source while both are nearly at rest in the plastic source material. In this case one can use the time-stamped NaI(Tl) scintillator pulse integrals (Fig. 4) with SDE time-to-digital converter (TDC) and 2D MCA modules in post-processing to identify both coincident and non-coincident gammas and determine their energy spectra. Detectors placed at  $90^\circ$  and other angles relative to each other can then verify that the two

coincident gammas are emitted back-to-back ( $180^\circ$  apart). Post-processing SDE software written in PYTHON (by UM undergraduate student ND) was used to generate 2D MCA plots, where the coincident gamma spectra along with random coincident events can be displayed (Fig. 5). As shown in Fig. 5, the coincident gamma photo-peaks are determined to each be 511 keV. However, we note that coincident Compton scattering of the 511 keV gammas in the NaI(Tl) detectors also is observed (Fig. 5) along with some random coincident events as pile-up rejection was not implemented. Such 2D data visualization, which can be highly educational, requires multi-parameter coincident data acquisition and display (SDE 2D MCA), not easily done with conventional electronics and single-channel (1D) pulse-height analyzers.

#### B. Application: PET medical imaging

This experiment serves to introduce students to a highly effective physics-based modality in medical imaging,

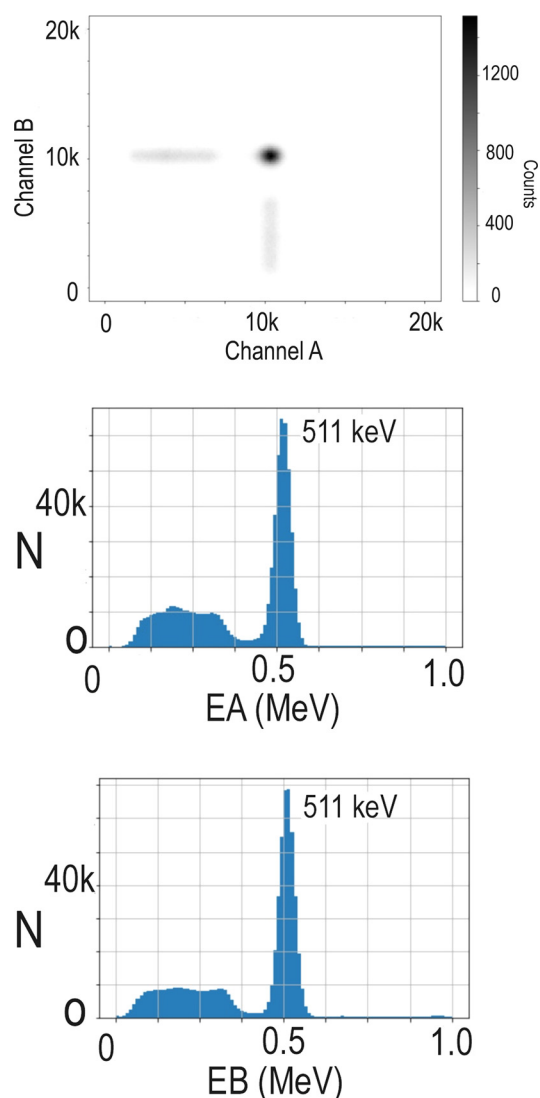


Fig. 5. Top: 2D coincident Na-22 NaI(Tl) gamma-ray digitized pulse integral spectra in two detectors, denoted as detector A and detector B, generated using student-written post-processing Python 2D MCA SDE. Bottom: The projected SDE NaI(Tl) calibrated energy spectra (SDE 1D MCA) in the corresponding detectors observed for the two coincident Na-22 annihilation gamma rays detected  $180^\circ$  apart.

positron-emission tomography (PET). As seen in Fig. 5, a positron-emitting source can readily be identified via the detection of coincident 511 keV annihilation gamma rays, as these provide a unique signature. Using suitably collimated detectors, the location of the annihilation, which could be a cancer tumor, can be located to a few mm, e.g., 2–5 mm depending on the radioisotope employed<sup>18</sup> (see also: Wikipedia “Positron emission tomography” and references cited there). PET imaging uses short-lived positron-emitting radioisotopes such as C-11, N-13, O-15, F-18, Ga-68, Zr-89, and Rb-82 incorporated into special radio-pharmaceuticals. The latter accumulate in one or more organs in the body having specific medical problems. The PET images then provide both static images as well as physiological information, e.g., the uptake rate of the radio-pharmaceutical.<sup>18</sup> This can facilitate discovery and treatment of cancer tumors at an early stage, detection and analysis of cardiovascular and neurological disease, etc.<sup>18</sup> This imaging modality has low background as it requires, as illustrated above, the detection of two coincident 511 keV positron-annihilation gamma rays. Hence very low amounts of radioactive material with minimal radiation dose to a patient are needed to obtain a good image.<sup>18</sup>

### C. Co-60 gamma-gamma coincidence (SDE 2D MCA)

The radioactive nucleus Co-60 beta decays with a half-life of 5.26 years to excited states of Ni-60 (see Ref. 6, Expt. 19). The  $J^\pi = 4^+$ ,  $E_x = 2.51$  MeV Ni-60 excited state (recall  $J$  is the spin and  $\pi$  is the parity of the level) decays sequentially in coincidence with the decay of the  $J^\pi = 2^+$ , 1.33 MeV excited state to the  $J^\pi = 0^+$  ground state of Ni-60. This produces two prominent coincident gamma rays at  $E = 1.17$  MeV and 1.33 MeV (see Ref. 6, Expt. 19). Coincident gamma-ray studies have proved especially important in studying and identifying nuclear levels, especially in deformed nuclei where the level spacing, often up to  $J^\pi > 50^+$  levels (!), can be used to deduce nuclear moments of inertia.<sup>19,20</sup> Most of these experiments now use very large arrays of gamma-ray detectors together with high-speed pulse digitizers.<sup>21</sup> Such experiments have revealed some dramatic and unexpected results regarding nuclei.<sup>19–21</sup> Gamma-gamma coincidence is an important nuclear experimental technique studied in most advanced teaching labs<sup>10</sup> and is readily demonstrated with the SDE system described here.

The setup for this experiment again consists of two NaI(Tl) scintillators, denoted as detectors A and B, and PMTs (used to generate gamma-ray energy-related signals  $E_A$  and  $E_B$ ) set at specific angles relative to a Co-60 source. In the present case a modest, hence low-cost, US-NRC exempt 1.9  $\mu$ Ci Co-60 source was used together with two lead-shielded 2 in. long by 2 in. dia. NaI (Tl) detectors. These were set 180° apart and 3–4 cm each from the source, similar to the setup used for the Na-22 coincidence experiment (above). The coincidence timing was checked using the DSO mode in the digitizer together with a Na-22 source, although in some cases this can also be done using a split signal from a Phillips Scientific Model 417 high-speed pulser (Phillips Scientific, Mahwah N.J.) to simulate the detector PMT anode pulses. The PMT HV to each detector was adjusted so the detector gains were approximately matched, but in any case, the energy spectra derived from the PMT anode pulse integral, using a 400 ns pulse-integral gate (long gate, Fig. 3), could be determined in units of MeV using

Na-22 and other known gamma-ray energy calibration sources. The on-board digitizer coincidence timing window was then set (40 ns wide) to ensure primarily fast coincidence data were recorded along with any random coincidences also falling within that window.

Random, overlapping coincidences, as observed using the digitizer’s two-channel DSO mode, initially proved to be an issue, and it was necessary to implement the user-defined on-board pulse pile-up rejection (PUR) SDE supplied by CAEN. This proved effective in eliminating most double pulses within each detector’s pulse-integral 400 ns wide gate window. PUR then allows one to count at relatively high rates (a few kHz) with minimal random coincidences or single-detector pulse pile-up in the spectra. Excessive low-energy events can be removed with the user-defined threshold settings in the FPGA, which specify the lowest voltage signals to be further digitized. This permits students to use close detector geometry and employ exempt-level radioactive sources (here a 1.9  $\mu$ Ci Co-60 source) to obtain sufficient coincidence data (Figs. 6 and 7). Since the sequential decays in Ni-60 occur within picoseconds (see Ref. 6, Expt. 19), the two gamma rays in the decay to the ground state (g.s.) appear to occur simultaneously in the NaI(Tl) detectors. However, there is still a small number of random events in the NaI(Tl) coincidence window, which appear as coincident events in the 2D and gated spectra (Figs. 6 and 7) but are from two different nuclear decay events that yet occur within the coincidence timing window.

A PYTHON SDE 2D-MCA routine was written (again by UM student ND) to display both coincidence gamma rays and any random coincidences together with gamma rays outside of the coincidence window. A 2D plot ( $E_A$  vs  $E_B$ ) of the detected gamma-ray energies (online color) is shown in Fig. 6. and confirms that the 1.17 MeV and 1.33 MeV gamma rays occur in coincidence, as allowed by the selection rules for gamma-ray decay for the levels involved (see Ref. 12, Chap. 10). Both the photo-peaks, along with the corresponding Compton spectra for these gamma rays, are observed. There also is indication of some 1.33 MeV and 1.17 MeV events due to decays from different nuclei that nonetheless

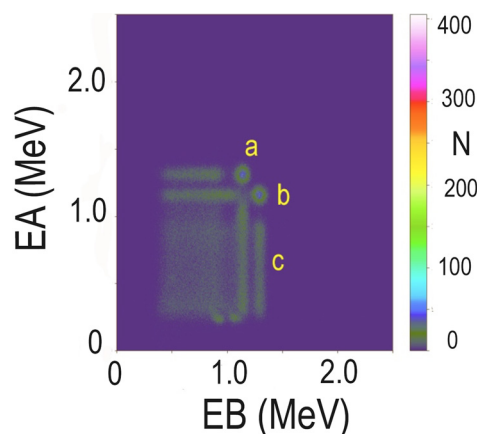


Fig. 6. A 2D energy spectrum ( $E_A$  vs  $E_B$ ) of pulse-integrated signals from a Co-60 source observed with two NaI(Tl) gamma detectors (denoted A and B) run in coincidence, 180° apart (SDE 2D MCA). Two strong Ni-60 gamma decay groups are indicated in coincidence in separate detectors, at 1.17 MeV and 1.33 MeV. Group a: 1.33 MeV gamma in detector A in coincidence with 1.17 MeV gamma in detector B; group b: 1.17 MeV gamma in detector A in coincidence with 1.33 MeV group in detector B; group c: Typical coincident Compton events in the detectors.



occur within the coincidence window. Projections onto the energy axes of one detector showing all coincident events as well as only 1.33 MeV gammas coincident with 1.17 MeV gammas are shown in Fig. 7.

As another part of this experiment students can measure the angular correlation between the two gamma rays, which is related to the nuclear spins and multipolarity of the levels. The correlation for the decay gammas from the two Ni-60 levels is fairly uniform versus angle, however (see Ref. 6, Expt. 19).

#### D. Random coincidences and dead-time measurements (DSO mode)

The digitizer SDE DSO mode allows students to observe random coincidences between two detectors, i.e., events in two detectors not in precise time coincidence. This can be studied in more detail by changing the user-defined coincidence timing gate width (see above). Likewise, pulse pile-up in the detectors can be studied using different source-detector distances, hence count rates, or a random-pulse generator and observing the errors introduced in the pulse integrals or related effects (see Ref. 10, Chap. 5).

#### E. Compton scattering (SDE TDC, 1D- and 2D-MCA)

Compton scattering is another important advanced nuclear-physics lab experiment that requires a fast coincidence measurement, in this case between a scattered gamma ray and the recoil electron (see Ref. 10, Sec. 2.7.2; Ref. 6, Expt. 10). This is readily done with a two-channel fast digitizer and vendor-supplied, student- or instructor-developed

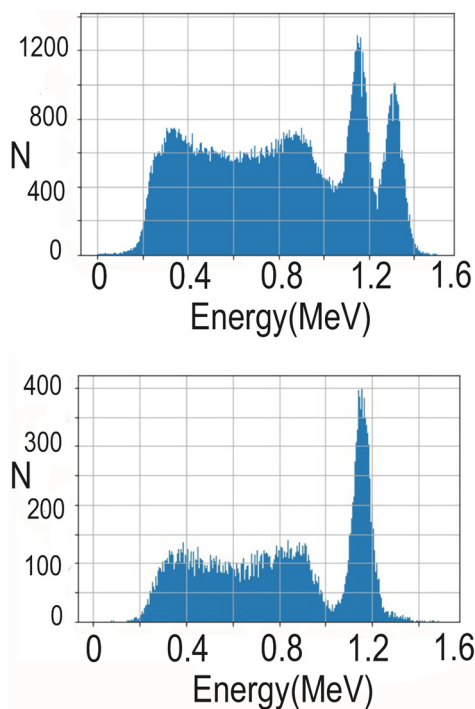


Fig. 7. Projected coincident Ni-60 gamma-decay spectra from a Co-60 source (Fig. 6) observed in one of the NaI(Tl) detectors (SDE 1D MCA). Top: All coincident events showing that the 1.17 MeV and 1.33 MeV gamma rays are in coincidence. Bottom: Projected spectrum (SDE 1D MCA) in the same detector but requiring coincidence with a 1.33 MeV gamma in the second detector, confirming the 1.17 MeV gamma is part of a fast gamma decay sequence between nuclear levels in Ni-60.

SDE TDC, 1D-, and 2D-MCA modules. A standard Compton scattering setup can be used,<sup>5-9</sup> with a plastic scintillator and PMT serving as the recoil-electron detector and a NaI(Tl) with PMT serving as the detector for the Compton-scattered gamma ray (Fig. 8). The coincidence timing window and energy calibrations are done as previously described. SDE post-processing software, which can be student-written as done here, is then used to create SDE 1D- and 2D-MCAs, a SDE TDC and other modules for visualization of coincident and non-coincident scattered gamma rays and recoil electrons. In this case, there is a direct correlation between these energies and the gamma-ray scattering angle via the well-known Compton relation.<sup>11-14</sup> The latter requires that the summed energy be equal to the incident gamma ray energy, in this case 662 keV (Cs-137). After calibrating the detectors with gamma-ray sources, data were obtained over several gamma scattering angles in the range from 30° to 90° (Fig. 9). This was done with (roughly) 2 in. × 2 in. diameter plastic and NaI(Tl) detectors using a 288  $\mu$ Ci collimated Cs-137 source. This is a strong, non-exempt source, but if longer running periods are available the experiment can be done with close-in geometry and exempt sources of a few  $\mu$ Ci (see Ref. 6, Expt. 19). Likewise, four-channel digitizers (CAEN DT5720 and XIA PIXIE-Net) would permit measurements at several gamma-ray scattering angles simultaneously, thus greatly expediting measurements.

Two-dimensional coincidence data spectra (SDE 2D MCA) summed over the gamma scattering angles measured are shown in Fig. 10. As predicted by the Compton equation, the scattered gamma ray and recoil electron energies are correlated and sum to 662 keV (within uncertainties) at all the gamma-ray scattering angles measured. As shown, this can be readily verified and visualized with appropriate SDE modules using the digitized coincident output data from a digitizer.

#### F. Related experiments utilizing multi-channel digitizers

As an additional part of the above experiment, students can also measure the gamma-ray Compton scattering probability versus scattering angle and verify the prediction of the Klein-Nishina theory derived from quantum electrodynamics (see Ref. 12, p. 200). This measurement, however, requires further information, such as the acceptance and detection efficiency of the two detectors as a function of the gamma ray or recoil electron energy.<sup>10,16,17</sup>

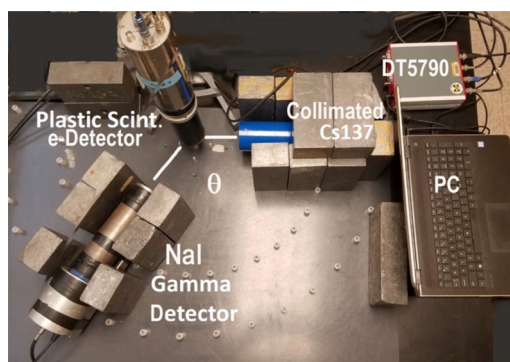


Fig. 8. Compton scattering setup as used with the CAEN DT5790N digitizer/HV supply and a collimated 0.288 mCi Cs-137 gamma source (Refs. 5-9).

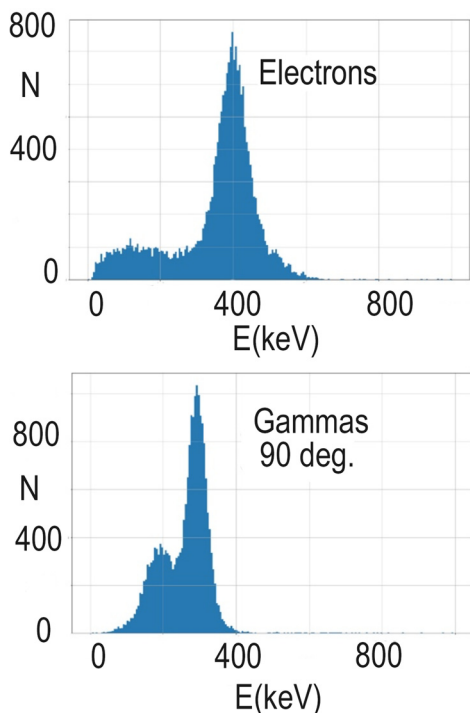


Fig. 9. Electrons (top) detected in a plastic scintillator (Fig. 8) in coincident with gamma rays (bottom) scattered at  $90^\circ$  and detected with a NaI(Tl) scintillator, as measured using 1D MCA SDE.

In these and other measurements, having a four-channel digitizer (CAEN DT5720 or XIA PIXIE-Net) with four detectors running simultaneously can be advantageous. Likewise, four detectors would expedite measuring the angular correlation in gamma-gamma coincident decays (e.g., Co-60; Ref. 6, Expt. 19), but also for measuring the angular distribution in alpha-particle Rutherford scattering (see Ref. 6, Expt. 15), and other experiments.<sup>5–10</sup> This could permit these experiments to be done in a single lab period in many cases yet still using US- NRC exempt low-intensity radioactive sources.<sup>5–9</sup>

### G. Muon lifetime (SDE TDC and 1D MCA)

Another important experiment is measurement of the cosmic-ray muon lifetime (see Ref. 11, Sec. 9.5).<sup>22</sup> This experiment illustrates Einstein's theory of relativity, e.g.,

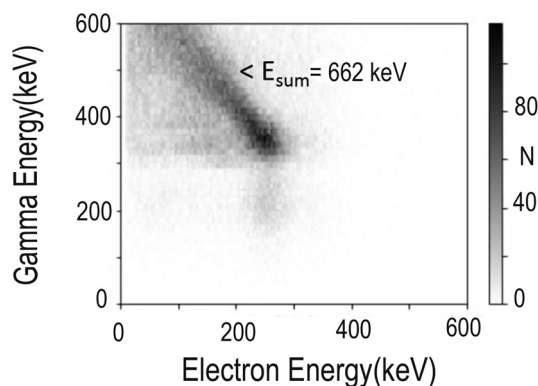


Fig. 10. SDE-generated 2D plot (2D MCA SDE) of coincident recoil electron and Compton-scattered gamma energies (Fig. 9) summed over several gamma-ray scattering angles,  $30^\circ$  to  $90^\circ$ .

time dilation in our reference frame and length contraction in the muon reference frame given that muons are produced in the upper atmosphere and would otherwise decay before reaching the Earth. The experiment can introduce students to topics such as DNA damage from cosmic rays, DNA repair via double strand DNA, and the time scale for evolution (see, e.g., Wikipedia and references cited there). It also introduces students to heavy leptons and the Standard Model of physics.<sup>11–14</sup>

In this version of the experiment, a simplified version of a standard setup (e.g., Ref. 8) can be used as the needed data can be obtained from a single PMT detector.<sup>22</sup> The original muon decay detector used by our students<sup>8</sup> consists of a large drum of oil scintillator with two large (5 in.) PMTs and associated electronics to trigger on any incident muon stopped in the scintillator. One PMT signal is used to trigger on the incident muon and a second PMT to trigger on the muon decay signal with a fast time measurement between them. This can now be done using only one PMT with just the digitizer/HV supply unit and suitable post-processing SDE TDC. The only requirement is that a wide digitizing window is specified ( $> a$  few  $\mu s$ ) such that both the incident and decay pulses are observed together, then digitized and recorded as event-mode data (12 bits, 250 MS/s). The post-processing SDE can then be written to locate the incident and decay signals (Fig. 11) and generate the time observed for the muon to decay when stopped via SDE TDC and 1D MCA modules. As noted, most digitizers can be operated remotely or in stand-alone mode, and data accumulated beyond the normal lab period to obtain good statistics (as done here). The mean lifetime of the muon when stopped (neglecting some small QM effects<sup>5–9</sup>) after correcting for random decay pulses (a constant background in the decay spectrum) can then be determined accurately (Fig. 12).

Since one large scintillator can accommodate several PMTs (as in the UM setup noted above in Ref. 8) and only a single digitizer is needed to acquire the needed PMT data, several students can be running the muon lifetime experiment using different PMTs at the same time, if appropriate.

### H. Fission-neutron time of flight (SDE TDC and 1D MCA)

This experiment is done with a sealed, depleted oil-well-logging Cf-252 spontaneous fission source, as described in Ref. 23. The SDE version replaces many analog electronics modules (NIM or CAMAC) with the CAEN two-channel

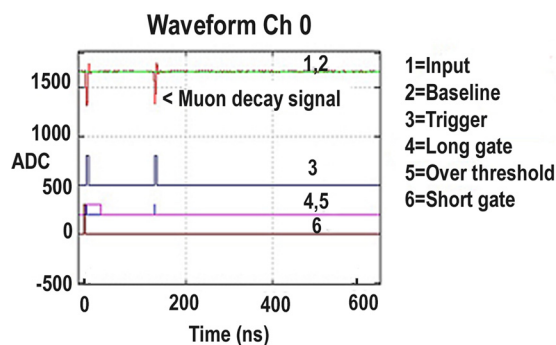


Fig. 11. Typical incident cosmic-ray muon (see Ref. 11, Sec. 9.5) and associated stopped-muon decay pulses as recorded in a digitizer data acquisition SDE DSO window.



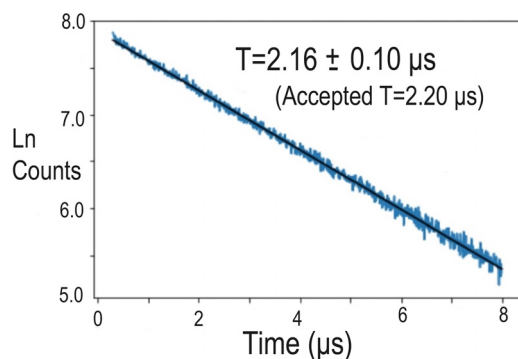


Fig. 12. SDE 1D-TDC time spectrum of stopped-muon decay data after background subtraction (uncorrected for small QM capture effects) indicating the fitted mean lifetime with uncertainty compared with the accepted intrinsic lifetime value (see Ref. 11, Sec. 9.5).

digitizer/HV supply operating in time-stamped list mode. In this mode, the signal from the start and stop plastic scintillators is recorded in the PC as a list of pulse integrals stored with a time stamp in 4 ns intervals (Fig. 4). SDE post-processing modules (in Python) written by one of us (ND) replacing analog coincidence and time-to-digital conversion (TDC) modules were then used to determine the time-of-flight (ToF) of the detected neutrons and gamma rays at the far detector. The scintillators were placed about 1 m apart (Fig. 13). The bottom scintillator is triggered by prompt gammas released in the spontaneous fission of Cf-252.<sup>23</sup> Typical time-of-flight data observed in the far detector as generated by SDE TDC post-processing software are shown in Fig. 14. The corresponding neutron energy spectrum

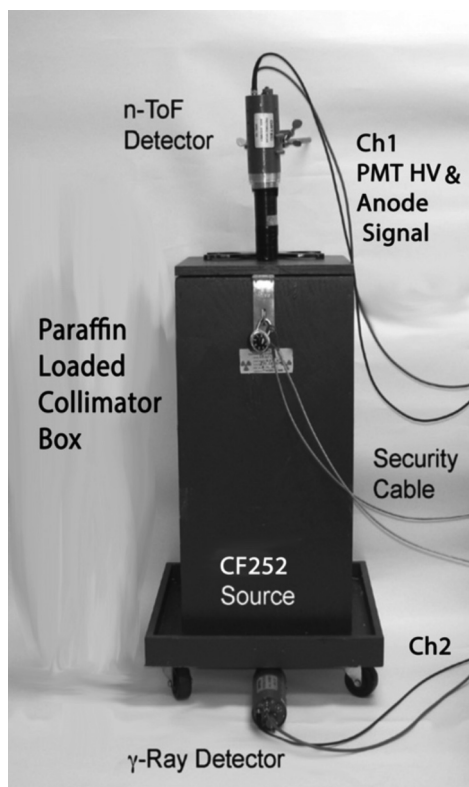


Fig. 13. Cf-252 fission neutron ToF setup (Ref. 23) with the plastic scintillator PMT HV and anode signals indicated for the two DT5790N digitizer channels.

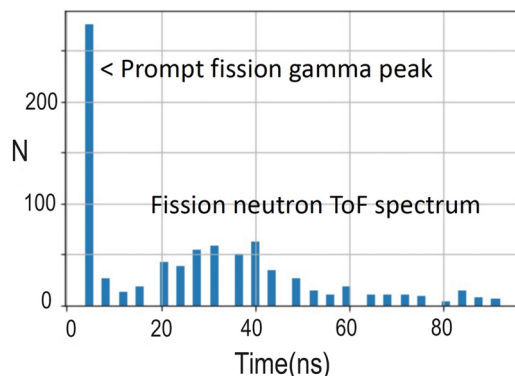


Fig. 14. Cf-252 fission ToF spectrum using a SDE TDC with the time-stamped scintillator data (Fig. 4). The zero-time value has been slightly offset for clarity.

deduced from the SDE TDC ToF spectrum (SDE 1D MCA), assuming non-relativistic kinematics since velocity  $v \ll c$ , is shown in Fig. 15.

As seen in Fig. 14, the prompt gammas that trigger the far detector occur well before the fission neutrons as, of course, the gammas travel at the speed of light  $c$ , whereas the neutrons are travelling at only a fraction of  $c$  with a kinetic energy of a few MeV.<sup>23</sup> While this particular digitizer has limited time resolution (4 ns intervals), the resulting ToF spectrum with a (roughly) 1 m flight path is sufficient to analyze the spectrum in terms of the expected Watt fission-neutron energy spectrum (Fig. 15) or other models.<sup>23,24</sup> However, depending on the age of the source, and especially if a depleted well-logging source is used, there can be some daughter isotopes in the source that produce high-energy fission neutrons and these can distort the ToF data<sup>25</sup> from that expected for a Watt fission-neutron spectrum (Fig. 15). As with other experiments, the data were accumulated over a long run-period using the event-mode data output option of the CAEN digitizer. This allowed us to use a depleted source within our US-NRC possession limits for Cf-252 (100 uCi).

The SDE TDC using time-stamped data even at 4 ns intervals can nonetheless yield timing resolution between a set of two detector pulses to 1 ns or less. This is possible if a large number of events are analyzed to give time distributions with accurate *mean* timing values<sup>10,16,17</sup> as the latter can be much better than the timing resolution for a single pair of events. The typical plastic scintillators used in this

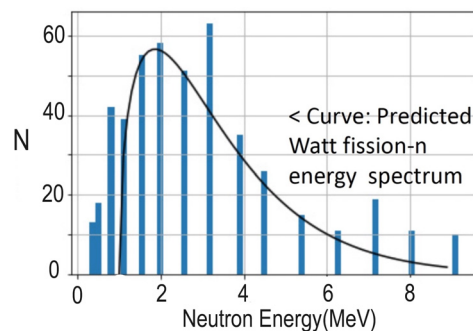


Fig. 15. Fission neutron energy spectrum (SDE 1D MCA) deduced from the ToF SDE TDC spectrum (Fig. 14). The curve shown is the predicted Watt energy spectrum for Cf-252 (Refs. 23–25). However, depending on the age of the Cf-252 source, the observed neutron energy spectrum can be slightly distorted due to fission of daughter nuclei (Ref. 25).

experiment do not allow for pulse-shape discrimination so the on-board vendor-supplied PSD SDE or student-developed PSD SDE cannot be used. But for the fission experiment, except for some delayed gammas, most gamma rays can be separated via their ToF using a user-written SDE TDC (Fig. 14). However, the use of certain liquid, crystalline or newer plastic scintillators which have PSD capability<sup>26,27</sup> could be utilized with on-board or user-developed SDE replacing the CAMAC modules used in Ref. 23 for PSD. In particular, in an organic liquid scintillator, neutrons can be separated from gamma-ray signals by using a pulse-shape identification (PSD) parameter based on the long and short integrated pulse gates (Fig. 3) together with the FPGA SDE software supplied by CAEN as an option<sup>1</sup> and similar software from XIA.<sup>2</sup> Electrons, muons (e.g., cosmic-ray muons), and charged particles can similarly be identified if needed using PSD in some cases.<sup>26,27</sup>

### I. SDE MCA and MCS applications

The simplest application of a pulse digitizer with vendor- or user-supplied SDE is for experiments requiring just 1D multi-channel analyzer (MCA) or multi-channel scaler timing (MCS) functionality. Examples of experiments for a SDE MCA are gamma-ray, beta-, and alpha-particle energy spectroscopy.<sup>5-9,28-30</sup> In this case, the vendor-supplied SDEs using the on-board FPGAs can often be used to give integrals of the digitized energy-related pulses from appropriate nuclear detectors. Energy spectra, with user-defined low-energy thresholds and PUR employed as needed, can then be generated, displayed, and recorded online.<sup>1</sup> Alternately one can apply user-written post-processing SDE to the event-mode data list sent to the host PC (Fig. 4). Conveniently, most digitizers have built-in base-line stabilization and corrections for zero offset available to optimize the energy spectra. A typical solid-state silicon detector will usually require a preamplifier, which will produce slow charge-to-voltage signals<sup>5,6,10</sup> that can still be post-processed and calibrated with suitable SDE to give energy spectra (SDE MCA). These preamps also often have fast timing output signals.<sup>5,6,10</sup> The latter can be appropriate for high-speed digitizing and, via pulse integration, produce useable energy spectra.

Digitizing HPGe gamma data<sup>6,7,10,16,17</sup> can be more problematic due to the limited resolution of modest-cost digitizers as used here (12 bit, i.e., 4096 channels for the CAEN DT5790, DT5720, and XIA PIXIE-Net units<sup>1,2</sup>). In this case for high-resolution spectroscopy requiring only 1D spectra acquisition,<sup>28-30</sup> it may be more appropriate to use a modern, compact high-resolution (8000 channels or more) digitizer or dedicated MCA unit. As an example, the Amptek 8000D MCA unit uses a modest speed 100 MS/s, 16-bit pulse digitizer and a dedicated software<sup>31</sup> to provide MCA and MCS functionality suitable for many experiments not requiring multi-parameter data acquisition. A similar MCA/MCS single-channel unit but lower resolution, the Avicenna RX1200 uses a 12-bit, 200 MS/s digitizer<sup>32</sup> together with an on-board FPGA to allow custom pulse processing. Due to the relatively low resolution data (a few %) from NaI(Tl) and plastic scintillators obtained from typical PMT anode or dynode signals, adequate MCA gamma-ray or particle spectra (see above) can usually be obtained for detectors with 12-bit digitizers, including the DT5790, DT5720, XIA PIXIE-Net, and other units such as the Avicenna digital MCA.<sup>32-36</sup>

MCS functionality, for example, to measure nuclear decay lifetimes (e.g., see Ref. 6, Expt. 14), is often readily available via time-stamped data (Fig. 4). Thresholds for the pulse inputs or pulse integrals can be set by users (including students as appropriate) using the on-board FPGAs and SDE DSO display, or in post-processing SDE, to select specific nuclear-decay pulses. Using the list-mode data and appropriate SDE in post-processing, one can then accurately measure nuclear decay lifetimes. Given the high sampling rates (e.g., on the order of MS/s), short lifetimes can be accurately measured, such as the 2.6 min Ba-137m 662 keV gamma-decay half-life using a Cs-137/Ba-137m generator.<sup>5,6,28,29</sup>

### IV. ALTERNATE, LOWER-COST DIGITIZERS, DSOs AND SDE APPLICATIONS

The cost of pulse digitizers will in general depend on the digitized pulse-bit resolution, the sampling rate, and additional features. In teaching-lab applications not requiring high-speed digitization, significant savings can be obtained using a lower-cost digitizer with lower than 200 MHz/s sampling rate. One such unit is the Red Pitaya StemLabs 125–14 digitizer.<sup>36</sup> The latter is well suited for SDE as it uses a FPGA with a two-channel 125 MS/s, 14-bit digitizer. Unlike the CAEN DT5790 units, this and most other digitizers require external HV and preamp detector power supplies often with an external digitizer power supply or instrumentation rack also needed. Likewise, low-cost programmable controller modules such as the Arduino UNO with external sensors have been employed for teaching,<sup>37</sup> but again these require separate power supplies, preamp circuitry, etc. Such controllers, digitizers, and FPGA units come with various degrees of functionality in the vendor-supplied or user-group SDE, including technical support, but many can be programmed to generate list-mode data that can be post-processed by students with custom SDE.<sup>36-38</sup>

We are presently evaluating several such units and related custom or other SDE with encouraging results (below). Many low-cost digitizers appear well suited for several introductory and advanced atomic, molecular, and other physics teaching-lab experiments not requiring high-speed or high-resolution pulse digitization.<sup>8,9,39</sup> In particular, together with several undergraduate students, an experiment on chaotic systems using a Red Pitaya digitizer<sup>3,36</sup> has been developed. Here again, the digitizer data are readily visualized using student-, instructor-, or other SDE-software to display various important features of chaotic motion in multi-parameter space. Details of the experiment and SDE software will be presented elsewhere.

Another type of digitizer, which often can be utilized for data acquisition in an advanced laboratory including many of the experiments described here, is a digital storage oscilloscope (SDE DSO).<sup>40</sup> These often have provisions for exporting digitized multi-channel data to a PC in a form suitable for implementation of post-processing user-defined or other SDE. Some external detector power supplies may still be needed and most DSOs are not as versatile in terms of programming on-board calculations compared with a digitizer having on-board user-accessible FPGAs.

### V. IMPLEMENTATION

While the experiments described here were done using SDE software primarily written by a senior undergraduate

student (ND), further evaluation by a wider range of students will be needed before wide-spread implementation in our advanced lab curriculum. This will determine what aspects of the SDE software programming will be required of the students and for what particular experiments this will be appropriate. In any case implementation of various SDE software programs, including vendor- or instructor-supplied SDE software developed for the CAEN two-channel (DT5790,DT5720), CAEN four-channel (DT5720), XIA PIXIE-Net four-channel, and Red Pitaya digitizers, is initially planned. This will provide our students with an introduction to modern high-speed pulse digitization and SDE. Although the present work utilized primarily a DT5790N digitizer with built-in HV supplies, the CAEN DT5720 digitizer, which lacks the HV power supplies, has the advantage that it can use the extensive CAEN-supplied CoPASS SDE software<sup>1</sup> and is available as a four-channel unit. The DT5720 digitizer and CoPASS SDE software are being evaluated at both UM and the University of Illinois for nuclear physics teaching lab purposes.<sup>41</sup> Also, the CoPASS SDE software is being modified by CAEN for use with the DT5790 digitizers.

As indicated, other research-level high-speed digitizers also may be adaptable for teaching applications with appropriate SDE (e.g., see Refs. 34 and 35). Likewise, there are several modest-speed low-cost digitizers, e.g., see Ref. 36, that utilize vendor- or user-supplied SDE that can be effectively employed in other types of teaching labs (atomic and solid-state physics, optics, and so on) not requiring high-speed, high-resolution digitizing or fast coincident signal timing.

## VI. CONCLUSIONS

Modern high-speed ( $>200$  MS/s) (Refs. 1 and 2) and many modest-speed digitizers (e.g., see Ref. 3), as demonstrated here, can effectively be used with appropriate vendor-supplied on-board, or user-written post-processing software-defined electronics (SDE) for advanced physics teaching labs, and in particular nuclear-physics experiments. The needed SDE can be student- or instructor-generated if appropriate using one of many common programming languages. The digitizer with suitable SDE can replace much of the conventional electronics and power supplies (e.g., NIM and CAMAC modules and power bins) used in many of these experiments. Multi-parameter data can readily be acquired and displayed allowing for highly visual multi-dimensional presentation and analysis of the data. Pulse digitizers and SDE introduce students to modern state-of-the-art physics data acquisition, signal processing, data visualization, and analysis as also used in many other areas of present-day scientific research.

## ACKNOWLEDGMENTS

This work was supported in part by REU supplement to NSF grant PHY 14-01242. This paper is based mostly on the work presented by one of us (N.D.) at the October 2018 Fall APS meeting (Ref. 42).

<sup>1</sup>CAEN Technologies, Staten Island N.Y. 10305, <[www.caen.it](http://www.caen.it)>.

<sup>2</sup>XIA LLC, Hayward CA 94544, <[www.xia.com](http://www.xia.com)>.

<sup>3</sup>Red Pitaya, <[www.redpitaya.com](http://www.redpitaya.com)>.

<sup>4</sup>John Essick, *Hands-On Introduction to LabVIEW for Scientists and Engineers*, 4th ed. (Oxford U.P., New York, 2019).

<sup>5</sup>Jerome L. Duggan, *Laboratory Investigations in Nuclear Science* (The Nucleus, Oak Ridge, TN, 1988).

<sup>6</sup>*Experiments in Nuclear Science*, AN34, 3rd ed. (Ortec-Ametek, Inc., Oak Ridge, TN, 1987), <[www.ortec-online.com](http://www.ortec-online.com)>.

<sup>7</sup>*Laboratory Manual: Nuclear Science Experiments with Digital Electronics* (Mirion Technologies, Hourseheads, NY, 2017), <[www.canberra.com](http://www.canberra.com)>.

<sup>8</sup>*Physics 441/442 Advanced Laboratory Notes* (University of Michigan, Michigan, 2018), <<http://instructor.physics.lsa.umich.edu/adv-labs>>.

<sup>9</sup>*Advanced Physics Laboratory Manual*, edited by J. W. Hammer (University of Notre Dame, Indiana, 2008), <[www3.nd.edu/~wzech/advancedphysicslab.html](http://www3.nd.edu/~wzech/advancedphysicslab.html)>.

<sup>10</sup>W. R. Leo, *Techniques for Nuclear and Particle Physics Experiments*, 2nd. revised ed. (Springer-Verlag, Berlin, 1994).

<sup>11</sup>Jeff C. Bryan, *Introduction to Nuclear Science*, 3rd. ed. (CRC Press, Boca Raton, FL, 2018).

<sup>12</sup>Kenneth S. Krane, *Introductory Nuclear Physics*, 3rd. ed. (John Wiley and Sons, N.Y. N.Y., 1988).

<sup>13</sup>Ernest M. Henley and Alejandro Gracia, *Subatomic Physics*, 3rd. ed. (World Scientific, Singapore, 2007).

<sup>14</sup>A. Das and T. Ferbel, *Introduction to Nuclear and Particle Physics*, 2nd. ed. (World Scientific, Singapore, 2003).

<sup>15</sup>Fairview Microwave, Lewisville, TX 75056.

<sup>16</sup>Glenn F. Knoll, *Radiation Detection and Measurement*, 4th ed. (John Wiley, N.Y., 2011).

<sup>17</sup>Nicholas Tsoulfanidis and Sheldon Landsberger, *Measurement and Detection of Radiation*, 3rd ed. (CRC Press, Boca Raton, FL, 2011).

<sup>18</sup>Gopal B. Saha, *Basics of PET Imaging*, 2nd ed. (Springer, N.Y., 2010).

<sup>19</sup>M. J. A. de Voigt, J. Dudek, and Z. Szymański, "High-spin phenomena in atomic nuclei," *Rev. Mod. Phys.* **55**, 949–1046 (1983).

<sup>20</sup>David Ward and Paul Fallon, "High spin properties of atomic nuclei," *Adv. Nucl. Phys.* **26**, 167–291 (2001).

<sup>21</sup>D. Weisshaar *et al.*, "The performance of the  $\gamma$ -ray tracking array GRETINA for  $\gamma$ -ray spectroscopy with fast beams of rare isotopes," *Nucl. Instrum. Meth. Phys. Res. A* **847**, 187–198 (2017).

<sup>22</sup>"Muon lifetime," TeachSpin, Buffalo, N.Y., <<https://www.teachspin.com/>>.

<sup>23</sup>F. D. Becchetti, M. Febraro, R. Torres-Isea, M. Ojaruega, and L. Baum, "<sup>252</sup>Cf fission-neutron spectrum using a simplified time-of-flight setup: An advanced teaching laboratory experiment," *Am. J. Phys.* **81**, 112–119 (2013).

<sup>24</sup>F. H. Frohner, "Evaluation of <sup>252</sup>Cf prompt fission neutron data from 0 to 20 MeV by Watt spectrum fit," *Nucl. Sci. Eng.* **106**, 345–352 (1990).

<sup>25</sup>F. D. Becchetti, "Comment on '<sup>252</sup>Cf fission-neutron spectrum using a simplified time-of-flight setup: An advanced teaching laboratory experiment [Am. J. Phys. **81**, 112–119 (2013)]'," *Am. J. Phys.* **82**, 206 (2014).

<sup>26</sup>F. D. Becchetti, R. S. Raymond, R. O. Torres-Isea, A. Di Fulvio, S. D. Clarke, S. A. Pozzi, and M. Febraro, "Recent developments in deuterated scintillators for neutron measurements at low-energy accelerators," *Nucl. Instrum. Meth. Phys. Res. A* **874**, 72–78 (2017).

<sup>27</sup>N. P. Zaitseva *et al.*, "Recent developments in plastic scintillators with pulse shape discrimination," *Nucl. Instrum. Meth. Phys. Res. A* **889**, 97–104 (2018).

<sup>28</sup>Sidney A. Katz and Jeff C. Bryan, *Experiments in Nuclear Science* (CRC Press, Boca Raton, FL, 2011).

<sup>29</sup>Randolph S. Peterson, *Experimental  $\gamma$  Ray Spectroscopy and Investigations of Environmental Radioactivity* (Spectrum Techniques, Oak Ridge, TN, 1996).

<sup>30</sup>F. D. Becchetti, M. Febraro, J. Riggins, and R. O. Torres-Isea, "A multi-functional apparatus for  $\alpha$  and  $\beta$  spectroscopy utilizing a permanent ring-magnet  $\beta$  spectrometer," *Am. J. Phys.* **84**, 883–893 (2016).

<sup>31</sup>MCA-8000D, Amptek, Inc., Bedford, MA 01730.

<sup>32</sup>RX1200 Digital Spectrometer, Avicenna Instruments LLC, Corvallis, OR 97330.

<sup>33</sup>UCS-30 and ICS PCI Computer Spectrometers, Spectrum Techniques LLC, Oak Ridge, TN 37830.

<sup>34</sup>Analog Devices EVAL-AD9680, <[www.analog.com](http://www.analog.com)>.

<sup>35</sup>Signatec-Dynamic Signals LLC, Lockport, IL 60441.

<sup>36</sup>StemLab 125-14 by RedPitaya, <[www.redpitaya.com](http://www.redpitaya.com)>.

<sup>37</sup>C. M. Lavelle, "Gamma ray spectroscopy with the Arduino UNO," *Am. J. Phys.* **86**, 384–394 (2018).



- <sup>38</sup>Geza Kolumban, “Software defined electronics: A revolutionary change in design and teaching paradigm of RF radio communication systems,” *ICT Express* **1**, 44–54 (2015).
- <sup>39</sup>Adrian C. Melissinos and Jim Napolitano, *Experiments in Modern Physics*, 2nd ed. (Academic Press, NY, 2013).
- <sup>40</sup>Jason Engbrecht and Nathaniel Hillson, “A flexible positron spectrometer for the undergraduate laboratory,” *Am. J. Phys.* **86**, 549–558 (2018).

- <sup>41</sup>Prof. A. Di Fulvio, University of Illinois, Department of Nuclear Engineering (private communication, 2019).
- <sup>42</sup>Nathan Damron, Frederick D. Becchetti, and Ramon O Torres-Isea, “Applications of digital pulse acquisition systems and software defined electronics in advanced teaching labs,” *Bull. Am. Phys. Soc.* **63**, 12 (2018); <<http://meetings.aps.org/link/BAPS.2018.HAW.HA.80>>.
- <sup>43</sup>See supplementary material at <https://doi.org/10.1119/1.5125128> for digitizer and SDE-related information including sample SDE programs.



### Electric Fly

When this device is connected to a Wimshurst machine or other electrostatic generator, the arms begin to revolve with the points facing to the rear. The presence of the highly-charged points results in a locally-large electric field, and charge flies off the points. This gives a kick to the apparatus, and it revolves. A nice demonstration: easily built, entertaining as well as being scientifically interesting and not often used today. This apparatus is at the physics department at the University of Utah. (Picture and text by Thomas B. Greenslade, Jr., Kenyon College)